Cent. Eur. J. Phys. • 9(6) • 2011 • 1452-1457
DOI: 10.2478/s11534-011-0064-x

VERSITA

Central European Journal of **Physics**

Situations in traffic - how quickly they change

Research Article

Małgorzata J. Krawczyk[1*], Cristina Beltran Ruiz[2†], Krzysztof Kułakowski[1‡]

1 *Faculty of Physics and Applied Computer Science, AGH University of Science and Technology, al. Mickiewicza 30, PL-30059 Kraków, Poland*

2 *Sociedad Iberica de Construcciones Electricas, C/Sepúlveda 6, 28108 Alcobendas, Madrid, Spain*

Received 16 December 2010; accepted 27 June 2011

Abstract: Spatio-temporal correlations of traffic intensity are analyzed employing data collected for the motorway M-30 around Madrid during one week in January 2009. We found that the lifetime of these correlations is the shortest in the evening between 6:00 p.m. and 8:00 p.m. This lifetime represents a new indicator for the amount of attention that is demanded by drivers in given traffic conditions.

PACS (2008): 01.30.-y, 01.30.Xx, 01.30.Tt

Keywords: traffic • data analysis • lifetime

© *Versita Sp. z o.o.*

1. Introduction

As an interdisciplinary application of statistical physics, the physics of traffic is not a new subject. As several problems in the physics of traffic remain to be solved, this research field is far from being exhausted. One of the central questions is how traffic jams arise and how to control them. In the context of these issues, various modeling approaches have been proposed [1–4]; they range from partial differential equations to cellular automata. As a general rule, two phases of traffic are discussed: free flow and jam. Apart from these two, a synchronized phase has been distinguished [5, 6]. The synchronized phase manifests itself as a two-dimensional cloud in the fundamental diagram (density ρ, intensity A) as shown in Fig. 1, whilst the free flow is characterized by an approximately linear plot: $A \propto \rho$. Three types of states have been identified with a synchronized phase: *i)* stationary and homogeneous states, where both average velocity and flow remain constant during long times, *ii)* states where only the average velocity is stationary, and finally *iii)* non-stationary and non-homogeneous states [5]. Later, the concept of a synchronized phase was criticized as being ambiguous [7]. According to this criticism, the above types of traffic states are qualitatively different, and therefore they cannot be classified as a specific phase. Still, synchronization has been frequently cited in Refs. [8–11]. To describe different traffic states, some specific order parameters have been introduced [10, 12], such as the mean density of triplets of correlated vehicles. Nevertheless, a model parameterization of traffic systems remains a challenge.

In this work, our aim is to investigate the mean lifetime of spatial configurations of moving vehicles. The motivation is, most briefly, that these lifetimes give information on the rates of transitions of the traffic system from one state

*E-mail: gos@fatcat.ftj.agh.edu.pl
†E-mail: cbeltran@sice.com
‡E-mail: kulakowski@novell.ftj.agh.edu.pl

to another. Specific configurations of vehicles with their velocities can be treated as microscopic states. This kind of data is hardly available; more often coarse-grained data are collected as intensities A averaged over some time period, 30 seconds at best. From readings $A_1(t)$ and $A_2(t)$ collected with two sensors 1, 2 at a distance x one from another, we evaluate the time average of the correlation between $A_1(t)$ and $A_2(t+\tau)$. When the coarse-grained state changes only slightly in time, the correlation should show a maximum at the delay $\tau = x/v$, where v is the mean velocity of vehicles. We also note that the velocity spread of vehicles is expected to lead to a finite length of spatial correlations of A. The latter, rescaled again by v, is a measure of the lifetime of the coarse-grained states. An obvious shortcoming of this procedure is that the time of measurement (1 minute) is not commensurate with the mean time x/v of the motion of vehicles from one sensor to another. However, this difficulty can be evaded at least partially by averaging over more pairs of sensors.

The lifetime seems to be a new tool in the sense that we are not aware of its previous application for spatio-temporal correlations of traffic flow. In Ref. [13], autocorrelations in the free-flow, synchronized, and congested phases were investigated for the local density, the average velocity, and the flow. The autocorrelation functions measured with one sensor showed a slow decrease of density and flow in the free-flow state and a much quicker decrease in the synchronized state. In the congested (stop-and-go) state, the autocorrelation functions oscillate in time (see Figs. 10 and 12 in Ref. [13]). According to Ref. [6], the sequence of phases from the free-flow to the jammed phase is through the synchronized phase. On the other hand, an exemplary time series with a transition from the free-flow to the congested phase, studied in Ref. [13] (Fig. 13), shows a sharp transition, with only a momentary increase of the variance of the velocity. Both the short time of the transition and the short timescale of the autocorrelation functions can be due to the metastable character of the synchronized state. Data on the lifetime should provide information on how quickly the traffic states change.

In the next section, we give the details for our traffic data. The two subsequent sections are devoted to the calculations and to the numerical results. The last section contains our conclusions.

2. Data collection

The data are collected from one-minute aggregated readings of 24 sets of sensors or measurement points placed along a 13-km stretch of road on the M-30 motorway,

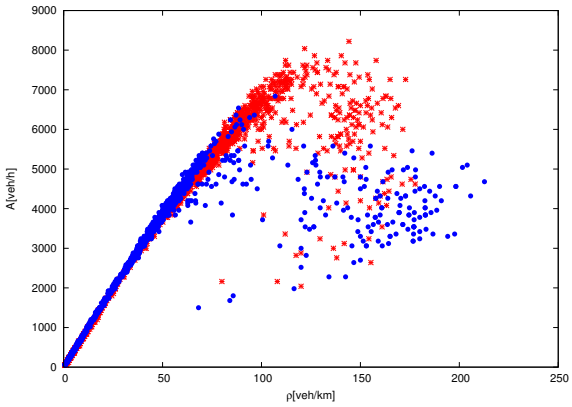

Figure 1. The fundamental diagram for two sensors (marked as $*$ and $\bullet$) on the motorway M-30 for a typical workday.

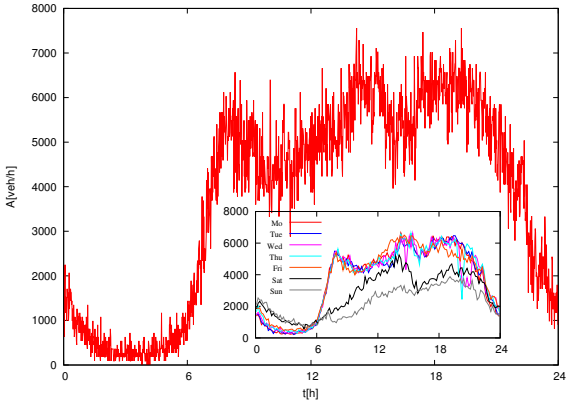

Figure 2. Intensity versus time as read by one sensor on the motorway M-30 for a 24-hour period (exemplary curve, all data) on a typical workday. The inset shows the curves for each day of the week; for clarity, the data are arranged in 10-minute bins. It is apparent that the data show different behavior for workdays and during the weekend, but the data do not appreciably differ between the individual workdays.

which surrounds the center of Madrid. The data sets cover the one-week period between January 26th and February 1st, 2009. These real-traffic data sets provided by the detectors include (i) the counting of vehicles; (ii) the intensity or flow of traffic (vehicles per hour, veh/h); (iii) time of detection (time that the sensor is detecting the presence of a vehicle); (iv) the real-time vehicle velocity (km/h); and (v) the vehicle length and classification by categories (car, bus, van, truck, etc.). A detailed description of the data can be found in Ref. [14]. From these data sets, we only use the intensity and velocity measurements (ii) and (iv).

Our real-world traffic data sets from the M-30 motorway have been measured by a detection system based on inductive loops; these inductive sensors are used in

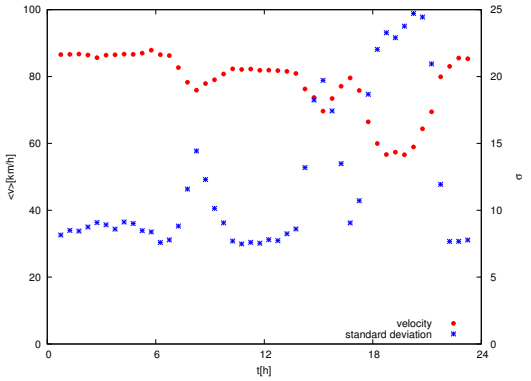

Figure 3. Velocity (red dots, left scale) and its standard deviation (blue stars, right scale) versus time on the motorway M-30 during a 24-hour time period. Both values are calculated as averages over workdays, over all sensors, and over half-hour time periods.

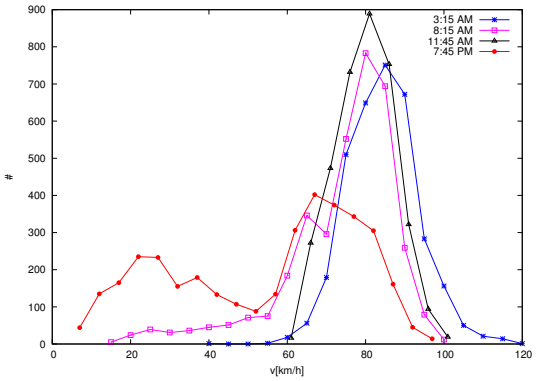

Figure 6. Velocity distribution for the four time periods centered at 3:15 a.m., 8:15 a.m., 11:45 a.m., and 7:45 p.m. Data for the histograms (number of cases versus velocity v) were collected within 30 minutes around the given time (e.g., 3:00–3:30 AM) from all sensors and during all workdays.

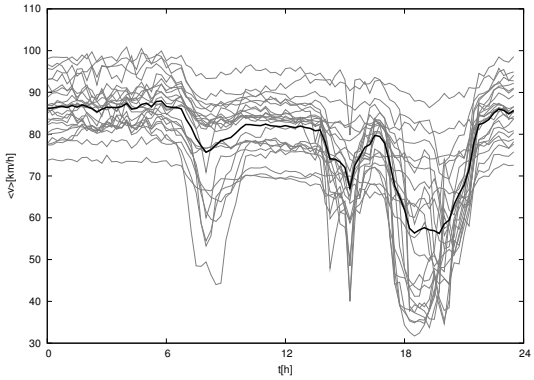

Figure 4. Velocity versus time on the motorway M-30 during a 24-hour time period as averages over workdays and over all sensors (black color) or averages over workdays for individual sensors (grey color) in 15-minutes time bins.

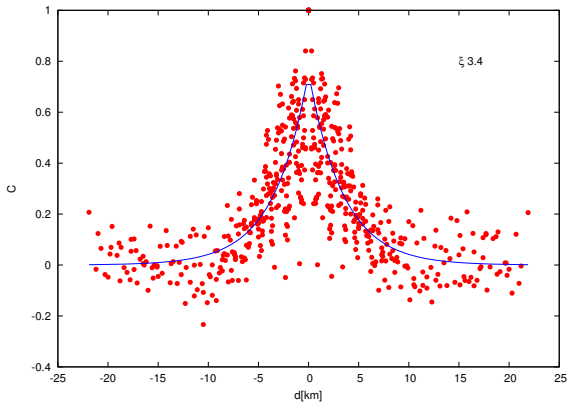

Figure 7. Correlation versus distance—an average over workdays for all pairs of 24 sensors between 4:00 a.m. and 4:30 a.m.on the motorway M-30. The blue line corresponds to the fitted curve.

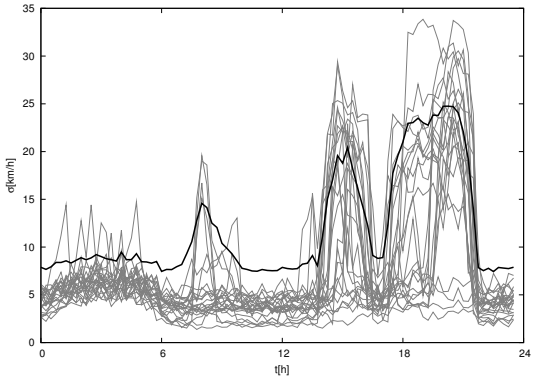

Figure 5. Standard deviation of velocity against time by 24 h in the motorway M-30 as an average over workdays and all sensors (black colour) or averages over workdays for individual sensors (grey colour) and a 15 minutes time periods.

detection systems that rely on the principle that a moving magnet—a vehicle—will induce an electrical current in a nearby conducting wire. This effect is applied for the detection of vehicle-presence indicators and thus for getting information on real-traffic data. The basis of these vehicle detection systems is the measurement of the induction change when a metallic mass (i.e., a vehicle) passes over a loop installed under the road pavement. The loop forms part of a circuit that oscillate at a determined frequency that is changed by the variations of the loop's inductance as the metallic mass passes over it. Then, the detector will translate the presence of a vehicle into an electrical signal that will be processed afterwards by a microprocessor that will digitally treat the obtained inputs transmitted by the induction loops so as to obtain real-traffic data. The de-

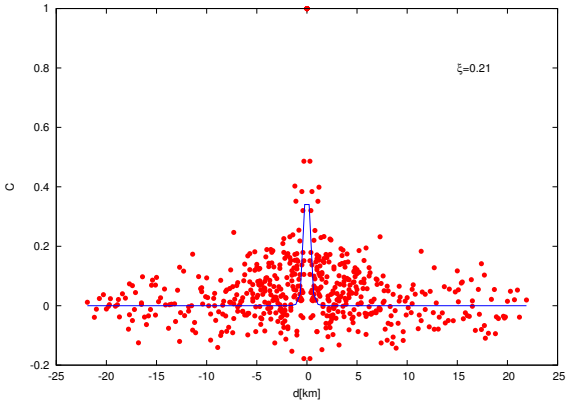

Figure 8. Correlation versus distance—an average over workdays for all pairs of 24 sensors between 6:00 p.m. and 6:30 p.m. on the motorway M-30. The blue line corresponds to the fitted curve.

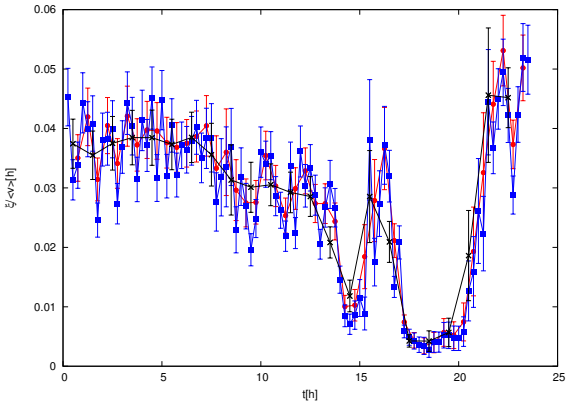

Figure 9. Lifetime $\tau = \xi/\langle v \rangle$ versus time. The average velocity is calculated as the average over workdays, over all sensors, and over time periods of 1 h, 30 min, and 15 min (crosses, dots, and squares, respectively).

tectors can aggregate real data upon different time bases. In the case of the M-30 motorway detection system, traffic data are aggregated on a one-minute integration period basis.

Detectors based on inductive loops are considered to be the most accurate electronic devices for vehicle detection; they are normally used in traffic detection due to their high robustness and reliability, their low sensitivity to adverse meteorological conditions, and their low cost. Therefore, the probability of erroneous vehicle sensing is very low. However, the detectors can suffer from shifts in their reference frequency, mainly due to large thermal changes in the pavement and from possible wire breaks or short-circuits.

3. Calculations

To verify the character of the data, the fundamental diagram of the data is reconstructed for two sensors, as shown in Fig. 1. The diagram displays the intensity A of traffic as a function of the vehicle density ρ. The value of the density ρ[veh/km] is calculated as the ratio A[veh/h]/v[km/h] at each point in time. As stated in the previous section, the data are registered every minute as an average value over the past minute.

For the remaining analysis, the time dependence of the intensity A is worked out. As is apparent from the inset of Fig. 2, the observed traffic data on workdays differ from those on weekends, a fact that is also intuitively understandable. Therefore, only data from workdays are taken into account in the subsequent calculations. The data in the inset also show that the shape of this curve is the same for all working days; see also the plots in Ref. [14]. In Fig. 3, we show the velocity and its standard deviation averaged over 30 minutes. It can be seen that a low velocity is correlated with a large variance.

The selected way of averaging does not change the character of the obtained results. As is apparent in Fig. 2, the curves for workdays are very similar. Also, a comparison of Fig. 3 with Figs. 4 and 5 illustrates that the time of averaging (30 and 15 minutes, respectively) can be changed without a significant influence on the results. The black curves in Figs. 4 and 5 show the results averaged over all 24 sensors, and the grey curves represent the data from the individual sensors.

The data $A(t)$ are subjected to detrendization [15]. The procedure is performed as follows: For each sensor and day the whole data set is divided into one-hour subsets. Each subset is fitted by a cubic function using the "least squares method." Subsequently, a value calculated on the basis of the parameters obtained from the fitting procedure is subtracted from each measured value. The procedure is applicable when the amount of data in a given time period is higher than the number of parameters of the function used for fitting, which is the case in the present context. Only data prepared in this way are used for further analysis.

We estimate the travel time between each pair of sensors (s_i, s_j) on the basis of the distance between them and the average velocity of vehicles in the given segment of the road. The average velocity is calculated as the average over workdays, over all sensors, and over half-hour time periods. After the estimated time period determined from this procedure, the same vehicles which were detected near the sensor s_i should then appear near the sensor s_j. Taking into account this time shift τ, the Pearson correlation coefficient c between a given pair of sensors

is given by:

$$c_{ij} = \frac{\sum_{t=1}^{n}(A_{it} - \bar{A}_i)(A_{j(t+\tau)} - \bar{A}_j)}{\sqrt{\sum_{t=1}^{n}\left(A_{it} - \bar{A}_i\right)^2}\sqrt{\sum_{t=1}^{n}\left(A_{j(t+\tau)} - \bar{A}_j\right)^2}}, \quad (1)$$

where A_{jt} is the intensity at the jth sensor for time bin t, and n is the length of the time series. Average values are calculated as $\bar{x}_i = \frac{1}{n}\sum_{t=1}^{n} x_{it}$ for one of the sensors considered and $\bar{x}_j = \frac{1}{n}\sum_{t=1}^{n} x_{j(t+\tau)}$ for the other. The obtained values c_{ij} lie in the range $[-1, 1]$, where $c_{ij} = -1$ means complete anti-correlation, $c_{ij} = 0$ a lack of correlation, and $c_{ij} = 1$ complete correlation. Each value is averaged with all other values obtained in the following 30 minutes. For all pairs of sensors and all time periods, the obtained values of the correlation coefficients are then averaged over workdays. Plotting all obtained data for half-hour time periods results in a curve that shows how the correlation coefficients depend on the distance between the sensors. Fitting this curve with a function $f(x) = \lambda \exp(-x/\xi)$, we obtain a correlation length ξ for each time period.

4. Results

The overall character of the fundamental diagram in Fig. 1 is similar to the fundamental diagrams reported in the literature [1–3]. Its left part shows an almost linear increase of the flow intensity (vehicles per hour) with the density (vehicles per km). More to the right we see a cloud of points, which is a consequence of traffic modes other than free flow.

As the data presented in Figs. 3, 4, and 5 show a distinct time dependence of the velocity, we checked the velocity distribution for selected time instants during workdays. The results are shown in Fig. 6 for 3:15 a.m., 8:15 a.m., 11:45 a.m., and 7:45 p.m. As we see, the distributions are unimodal except in the case of 7:45 p.m., where it is bimodal with a left maximum at around 20 km/h. The maximum on the right appears at approximately 65 km/h, and it overlaps with three other unimodal peaks. It is justified to state that the left maximum detected at 7:45 PM is related to a synchronized state. Note that the speed limit at this location is 90 km/h.

In Figs. 7 and 8, the plots show the data for the correlation coefficient c. These results, collected for all pairs of sensors, are averaged over workdays and fitted to extract the distance dependence of $f(d) = \lambda \exp(-d/\xi)$. The value of the obtained correlation length ξ is 3.4 km for the readings between 4:00 a.m. and 4:30a.m., and 0.21 km between 6:00 p.m. and 6:30 p.m.

Figure 9 shows the data for the lifetime τ of the spatial configurations defined as $\tau = \xi/\langle v \rangle$. It is remarkable that the increase of the intensity A of the flow between 6:00 a.m. and 8:00 a.m. and the minimum of the velocity $\langle v \rangle$ at 8:00 a.m. accompanied by a sharp maximum of the velocity's standard deviation σ influence the lifetime τ only slightly. Another decrease of v after 3:00 p.m. with an even sharper peak in σ can be correlated with irregularities of the lifetime τ. It is between 6:00 p.m. and 8:00 p.m. where we observe a qualitative drop of the lifetime τ. Simultaneously, the velocity's standard deviation σ gets a daily maximum of 25 km/h, as shown in Figs. 3 and 5.

5. Discussion

It follows from our results that the data collected from 6:00 p.m. to 8:00 p.m. describe states with the lowest mean velocity $\langle v \rangle$ and the shortest lifetime τ. In this time period, the velocity variance σ is at its largest value. This finding is of interest because of the notion that the velocity variance shows a maximum at the transition between the flow phase and the congested phase, where we expect the synchronized state. It was stated in Ref. [13] that the existence of this maximum is a numerical artifact of an appearance of two different phases within the same time interval. Our interpretation is that the large velocity variance marks a series of relatively rapid changes between different traffic states with two characteristic velocities marking a kind of slow-and-fast motion rather than stop-and-go. The short lifetime seems to be an apt characteristic of the varying state. It would be desirable to evaluate it also for traffic systems without ramps, where the dynamics is not influenced by external sources or sinks.

According to the statistics provided by the Insurance Institute for Highway Safety, it is between 5:00 p.m. and 7:00 p.m. when most people are killed in road accidents [1]. As we have seen in the presented data, the road conditions in these hours are: the largest traffic intensity, a moderate mean velocity, and the largest velocity variance. As noted above, the latter quantity is expected to be low in a synchronized phase of any kind, and—obviously—in the congested phase. The fact that between 6:00 p.m. and 8:00 p.m. the traffic configurations, as seen by drivers, change most quickly, can contribute to the deadly statis-

[1] *www.iihs.org/research/*

tics, as these quick changes demand the drivers' highest attention. It is likely that the lifetime proposed here provides a criterion for the evaluation and identification of potentially dangerous traffic states.

Finally, the lifetimes of particular traffic states, when handled within the theory of diffusion on networks [16], can be converted into rates of variations of time-dependent probabilities of microscopic and coarse-grained states of traffic systems. This kind of modeling, proposed recently in Ref. [17], seems to us particularly promising in applications to complex systems.

Acknowledgements

We thank the Madrid City Council for access to real data from the M-30 motorway. This research is partially supported within the FP7 project SOCIONICAL, No. 231288.

References

[1] D. Chowdhury, L. Santen, A. Schadschneider, Phys. Rep. 329, 199 (2000)
[2] D. Helbing, Rev. Mod. Phys. 73, 1067 (2001)
[3] K. Nagel, P. Wagner, R. Woesler, Operation Res. 51, 681 (2003)
[4] S. Maerivoet, B. De Moor, Phys. Rep. 419, 1 (2005)
[5] B.S. Kerner, H. Rehborn, Phys. Rev. E 53, R4275 (1996)
[6] B.S. Kerner, Phys. Rev. Lett. 81, 3797 (1998)
[7] M. Schönhof, D. Helbing, Transportation Res. Part B 43, 784 (2009)
[8] D. Helbing and B. A. Huberman, Nature 396, 738 (1998)
[9] H.Y. Lee, H.-W. Lee, D. Kim, Phys. Rev. Lett. 81, 1130 (1998)
[10] I. Lubashevsky, R. Mahnke, P. Wagner, S. Kalenkov, Phys. Rev. E 66, 016117 (2002)
[11] D. Helbing, K. Nagel, Contemp. Phys. 45, 405 (2004)
[12] I. Lubashevsky, R. Mahnke, Phys. Rev. E 62, 6802 (2000)
[13] L. Neubert, L. Santen, A. Schadschneider, M. Schreckenberg, Phys. Rev. E 60, 6480 (1999)
[14] A. Riener, K. Zia, A. Ferscha, C. Beltran Ruiz, J. Minguez Rubio, in 14th IEEE/ACM International Symposium on Distributed Simulation and Real Time Applications (DS-RT 2010), Fairfax, VA USA, (IEEE Computer Society Press, October 2010), p. 10
[15] J.W. Kantelhardt, E. Koscielny-Bunde, H. H. A. Rego, S. Havlin and A. Bunde, Physica A 295, 441 (2001)
[16] M.E.J. Newman, Networks. An Introduction, (Oxford UP, Oxford, 2010)
[17] M.J. Krawczyk, Physica A 390, 2181 (2011)